INFECTION AND IMMUNITY, Jan. 2011, p. 153–166 Vol. 79, No. 1
0019-9567/11/$12.00 doi:10.1128/IAI.00925-10
Copyright © 2011, American Society for Microbiology. All Rights Reserved.

Role of Purine Biosynthesis in *Bacillus anthracis* Pathogenesis and Virulence▽

Amy Jenkins,[1]† Christopher Cote,[1]† Nancy Twenhafel,[2] Tod Merkel,[3] Joel Bozue,[1] and Susan Welkos[1]*

Bacteriology Division[1] and Pathology Division,[2] U.S. Army Medical Research Institute of Infectious Diseases, 1425 Porter Street, Fort Detrick, Frederick, and Laboratory of Respiratory and Special Pathogens, Division of Bacterial, Parasitic, and Allergenic Products, CBER, FDA, Bethesda,[3] Maryland

Received 24 August 2010/Returned for modification 14 September 2010/Accepted 21 October 2010

***Bacillus anthracis*, the etiological agent of anthrax, is a spore-forming, Gram-positive bacterium and a category A biothreat agent. Screening of a library of transposon-mutagenized *B. anthracis* spores identified a mutant displaying an altered phenotype that harbored a mutated gene encoding the purine biosynthetic enzyme PurH. PurH is a bifunctional protein that catalyzes the final steps in the biosynthesis of the purine IMP. We constructed and characterized defined *purH* mutants of the virulent *B. anthracis* Ames strain. The virulence of the *purH* mutants was assessed in guinea pigs, mice, and rabbits. The spores of the *purH* mutants were as virulent as wild-type spores in mouse intranasal and rabbit subcutaneous infection models but were partially attenuated in a mouse intraperitoneal model. In contrast, the *purH* mutant spores were highly attenuated in guinea pigs regardless of the administration route. The reduced virulence in guinea pigs was not due solely to a germination defect, since both bacilli and toxins were detected *in vivo*, suggesting that the significant attenuation was associated with a growth defect *in vivo*. We hypothesize that an intact purine biosynthetic pathway is required for the virulence of *B. anthracis* in guinea pigs.**

Bacillus anthracis, the etiological agent of anthrax, is a spore-forming, Gram-positive bacterium (25, 52). The infectious form of *B. anthracis* is the spore, which under certain conditions may remain dormant for decades. Upon infection, spores are translocated to areas favorable for germination (53) into replicating bacilli, the form which ultimately kills the host (25, 52). While exogenous nutrients are required for the germination of the *B. anthracis* spore (53), the replicating bacilli are capable of synthesizing a majority of essential small molecules, as is evident by the presence of *de novo* biosynthetic enzymes in the *B. anthracis* genome (10, 41, 44, 48, 54). These molecules include purines, pyrimidines, vitamin cofactors, and amino acids.

De novo purine biosynthesis occurs by nearly the same pathway in most organisms, including bacteria, archaea, and eukaryotes (36, 72). In general, IMP is the first purine nucleotide formed in purine biosynthesis, with AMP and GMP derived from IMP in two additional catalytic steps each (Fig. 1A) (72). IMP is biosynthesized from 5-phosphoribosyl-α-diphosphate (PRPP) and L-glutamine in 11 catalytic steps. The final two steps in IMP biosynthesis are catalyzed by a single enzyme, PurH. PurH catalyzes the formylation of 5-aminoimidazole-4-carboxamide ribotide (AICAR) to give formyl-AICAR. In the final step, PurH catalyzes the cyclization of formyl-AICAR to IMP. IMP is then converted to AMP by PurA and PurB or to GMP by GuaB and GuaA (Fig. 1A). The IMP biosynthetic pathway is linked to the biosynthesis of thiamine through the intermediate aminoimidazole ribonucleotide (AIR) (Fig. 1A) (2). It should be noted that the *B. anthracis* biosynthetic transformations have not been determined experimentally but are based on genetic analysis of homologs in other organisms in which enzymatic activity has been verified experimentally (20, 46, 50, 72). The purine nucleotides described are used in many cellular processes (46); they are components of many coenzymes, involved in the regulation of metabolic pathways; and, most notably, they are the building blocks for nucleic acids.

In addition to the biosynthesis of purine nucleotides, many organisms are capable of salvaging purine nucleosides from their surroundings (3, 21). Purine salvage involves the uptake of purine nucleosides via a membrane-bound transporter. In the case of IMP in *B. anthracis*, inosine is transported into the cell and converted to hypoxanthine via a purine nucleoside phosphorylase (26). Hypoxanthine is then converted to IMP by hypoxanthine phosphoribosyltransferase (3, 21). There are a variety of pathways that can be utilized to convert salvaged purines. Therefore, while a bacterium incapable of producing IMP can be complemented with exogenous inosine, other purines in addition to inosine can also be utilized to overcome the deficiency. The salvage of purines can often be used to complement a loss of *de novo* purine biosynthesis depending on the availability of exogenous purines. While specific nucleoside transporters have not been well studied in *B. anthracis*, proteins homologous to those studied in model organisms, such as *Escherichia coli* and *Bacillus subtilis* (3, 21, 35, 56), are present in *B. anthracis.* The homology between these proteins suggests that *B. anthracis* has a similar capacity for nucleoside transport and salvage.

It has been shown that *de novo* purine biosynthesis is required for optimal virulence in a variety of pathogenic organisms, such as *Staphylococcus aureus* (47), *Streptococcus pneumoniae* (59), *Vibrio vulnificus* (37), *Salmonella enterica* serovar Typhimurium (29, 45, 63), and *Yersinia pestis* (8). *B. anthracis* auxotrophs requiring adenine, which contained mutations in

* Corresponding author. Mailing address: USAMRIID, Bacteriology Division, 1425 Porter Street, Fort Detrick, Frederick, MD 21702. Phone: (301) 619-9696. Fax: (301) 619-2152. E-mail: Susan.welkos@us.army.mil.
† A.J. and C.C. contributed equally to this work.
▽ Published ahead of print on 1 November 2010.

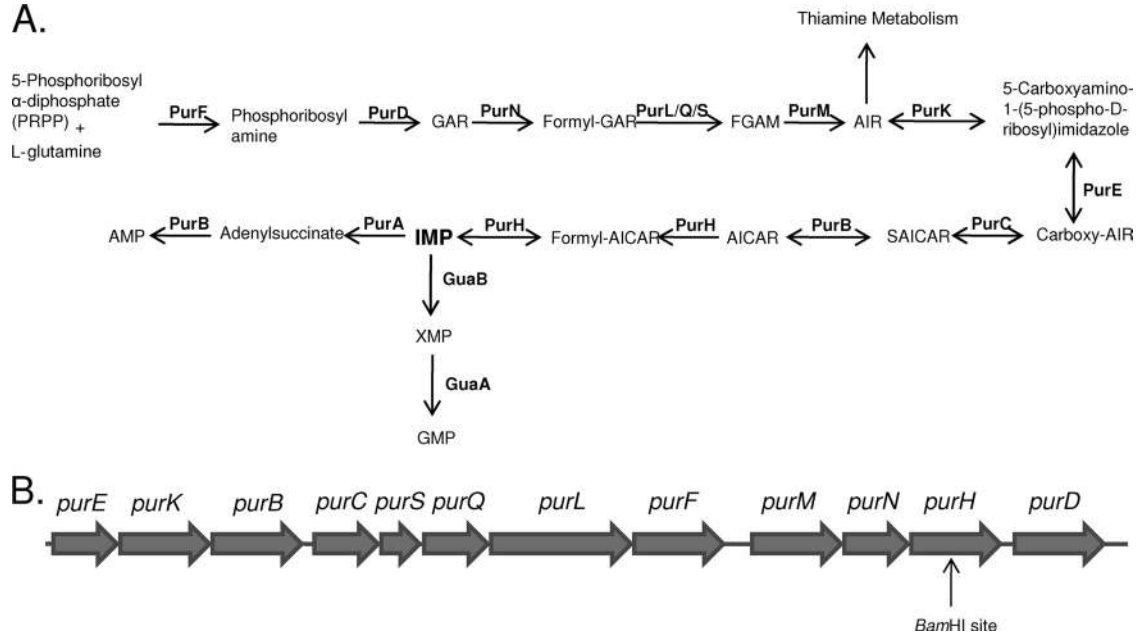

FIG. 1. (A) Purine biosynthetic pathway in *B. anthracis* as determined by *in silico* analysis with the KEGG database application. (B) Schematic representation of the gene arrangement of the purine biosynthetic operon in *B. anthracis*.

purA or *purB*, were found to be avirulent in a murine model of infection (30). In contrast, *B. anthracis* strains containing mutations in genes encoding enzymes further up the purine biosynthetic pathway, prior to the production of IMP, retained virulence in a murine model (30). Additionally, *B. anthracis* mutants deficient in guanosine biosynthesis (*guaA* mutants) retained virulence in a murine model by the intraperitoneal route of infection (30), suggesting differing roles for various purines in virulence.

In a screen of transposon libraries for mutants that exhibited altered phenotypes, we identified a mutation in the purine biosynthetic gene *purH*. The *purH* gene is the penultimate gene in the purine biosynthetic operon (Fig. 1B), rendering the *purH* mutant strain deficient in *de novo* purine biosynthesis, in particular in *de novo* IMP biosynthesis. Here we discuss the role of *de novo* purine biosynthesis in the virulence and pathogenesis of *B. anthracis* in several animal models of infection.

MATERIALS AND METHODS

Reagents, bacterial strains, and animals. The attenuated Sterne strain ($pXO1^+$ $pXO2^-$) and the fully virulent Ames strain ($pXO1^+$ $pXO2^+$) of *B. anthracis* were used in this study (40). *E. coli* strains DH5α and GM2163 were used in cloning and were obtained from Invitrogen (Carlsbad, CA) and New England Biolabs (Ipswich, MA), respectively. All restriction enzymes and ligases were obtained from New England Biolabs and were used according to the manufacturer's specifications. Polymerase was obtained from Invitrogen and Qiagen (Valencia, CA) (AccuPrime Pfx Supermix and Master Mix) and was used according to the manufacturer's specifications. The strains and primers used in this study are provided in Table 1 and Table 2, respectively. The following antibiotics were used: kanamycin (50 μg/ml for *E. coli*; 20 μg/ml for *B. anthracis*), ampicillin (100 μg/ml for *E. coli*), and erythromycin (5 μg/ml for *B. anthracis*). Female BALB/c mice were obtained from the National Cancer Institute (NIH-NCI, Frederick, MD) and were approximately 7 to 10 weeks old. Hartley guinea pigs (at least 350 g) and New Zealand White rabbits (approximately 3 kg) were obtained from Charles River Laboratories International (Wilmington, MA).

Identification of the mutant. The mutant of interest was isolated from a Tn*10* mutagenesis library in *B. anthracis* strain Sterne, and the site of transposon insertion was identified by rescue cloning (13). The transposon disruption occurred in a gene encoding a bifunctional protein annotated as IMP cyclohydrolase/phosphoribosyl aminoimidazolecarboxamide formyltransferase (PurH) (BAS0285). All work in this study was performed with the homologous protein in *B. anthracis* strain Ames (BA0298).

Construction of the *purH*::Kan mutant strain. The region encompassing the 1.5-kb *purH* gene and 500 bp upstream and downstream of the *purH* gene was PCR amplified from Ames genomic DNA. This 2.5-kb gene fragment was then cloned into KpnI/XbaI restriction sites in the *E. coli* shuttle vector pEO3 (7, 49). The resulting plasmid was then linearized by utilizing a native BamHI restriction site within *purH* (Fig. 1B). The *purH* gene was then interrupted by ligating the

TABLE 1. *B. anthracis* strains used in this study

Strain	Description	Source or reference
B. anthracis Ames	Fully virulent; $pXO1^+$ $pXO2^+$	40
B. anthracis Sterne	Attenuated; $pXO1^+$ $pXO2^-$	40
purH::Kan strain	*B. anthracis* Ames containing an Ω-Kan-2 fragment insertion in the *purH* gene	This paper
Δ*purH* strain	*B. anthracis* Ames containing an Ω-Kan-2 fragment replacement of the *purH* gene	This paper
Δ*purD* strain	*B. anthracis* Ames containing an Ω-Kan-2 fragment replacement of the *purD* gene	This paper
Δ*purH* + *purH* strain	Δ*purH* strain genetically complemented with native *purH* on the pEO3 plasmid	This paper
Δ*purH* + *purD* strain	Δ*purH* strain genetically complemented with native *purD* on the pEO3 plasmid	This paper
Δ*purD* + *purD* strain	Δ*purD* strain genetically complemented with native *purD* on the pEO3 plasmid	This paper

TABLE 2. Oligonucleotide primers used in this study

Description	Sequence
Upstream of *purH* (5′); used to construct *purH*::Kan and Δ*purH* mutants	5′-TGATAAACCGGTACCACGCGCTGTTGG-3′
Downstream of *purH* (3′); used to construct *purH*::Kan and Δ*purH* mutants	5′-ATAATCTCTAGAAGTTTCGTACGCTGCAGTTG-3′
purH screening primer (5′)	5′-CAATGGGGGCAAAGCACTATGAG-3′
purH screening primer (3′)	5′-ATCGCTACTGTTACACCTTTACCA-3′
Upstream of *purH* (3′); used to construct Δ*purH* mutant	5′-ACGCTTTTTCCCGGGTCCTTCACCCCTGGTTGTATG-3′
Downstream of *purH* (5′); used to construct Δ*purH* mutant	5′-TTCAAACACCCCGGGAGGAAGTTTAAAAAGTCCGG-3′
Upstream of *purD* (5′); used to construct Δ*purD* mutant	5′-ATTATTATGGTACCTTCTTTCT-3′
Upstream of *purD* (3′); used to construct Δ*purD* mutant	5′-TGCTACACCCGGGTTTTCTACTTT-3′
Downstream of *purD* (5′); used to construct Δ*purD* mutant	5′-TCGCCCGGGTTGAGAGTGATG-3′
Downstream of *purD* (3′); used to construct Δ*purD* mutant	5′-TCTCTAGAATTAAAGCGTGAGT-3′
capC (5′)	5′-ACTCGTTTTTAATCAGCCCG-3′
capC (3′)	5′-GGTAACCCTTGTCTTTGAAT-3′
pagA (5′)	5′-GTGCATGCGTCGTTCTTTGA-3′
pagA (3′)	5′-GCCGCTATCCGCCTTTCTA-3′
purH (5′); used to construct Δ*purH* + *purH* strain	5′-ATACAACCAGGGGTGAAGGTACCATGAAAAAGC-3′
purH (3′); used to construct Δ*purH* + *purH* strain	5′-AAACTTCCGTTTAAACTGTTTGAAATGACGTACG-3′
Upstream of *purH* (3′); SmaI site used to construct Δ*purH* + *purD* strain	5′-TGCACGCTTTTCCCGGGATCCTT-3′
pEO3-specific primer	5′-AAAAGTGCCACCTGACGTCTAAG-3′
purD (5′); used to construct Δ*purH* + *purD* strain	5′-TTCCCGGGTGAAATATGAATGTT-3′
purD (3′); used to construct Δ*purD* + *purD* and Δ*purH* + *purD* strains	5′-GGCTCTAGAAAAAGGTAAAT-3′
Upstream of *purD* (5′); used to construct Δ*purD* + *purD* strain	5′-GGTGGTACCCTCGTTCAA-3′
purD screening primer (5′)	5′-ATGCAGCGCTTAGTATCG-3′
purD screening primer (3′)	5′-TATTATTTTAGCCGCAGTTCTT-3′
Internal *purD* primer for RT-PCR (5′)	5′-CAAATACTGGCGGAATGG-3′
Internal *purD* primer for RT-PCR (3′)	5′-CTAGCCCTTTAATAATGTCACCTT-3′

Ω-Kan-2 fragment (57) into the BamHI site. The Ω-Kan cassette was utilized because it is stable and is constitutively expressed (57). In addition, through reverse transcription-PCR (RT-PCR) and complementation studies, we determined that any polar effect on the *purD* gene would be minimal. The plasmid was passaged through the GM2163 strain of *E. coli* before electroporation into *B. anthracis*. The Ames strain of *B. anthracis* was then electroporated with the pEO3-*purH*::Kan plasmid as described previously (13). The plasmid was integrated into the chromosome, and cointegrate clones were selected based on kanamycin resistance and temperature (42°C) resistance. Kanamycin-resistant clones were selected and streaked onto kanamycin plates (to screen for the presence of the Ω-Kan-2 fragment) and erythromycin plates (to screen for the presence of the pEO3 plasmid). Clones that were resistant to kanamycin but sensitive to erythromycin were screened for the presence of the resolved insertion mutation in the genome by PCR analysis.

Construction of the Δ*purH* and Δ*purD* mutant strains. The DNA flanking the *purH* or *purD* gene (~500 bp upstream and ~500 bp downstream of each gene) was PCR amplified using Qiagen Master Mix polymerase. The flanking regions were cloned into KpnI/XbaI restriction sites in the *E. coli* shuttle vector pEO3. The flanking regions were designed to produce a SmaI restriction site between the two regions. The Ω-Kan-2 fragment was inserted into the SmaI site, resulting in a complete replacement of the *purH* or *purD* gene with the Ω-Kan-2 fragment. The resulting plasmids were treated in the same manner as described above.

Genetic complementation. Two separate approaches were taken to genetically complement Δ*purH*. First, Δ*purH* was complemented with a full-length *purH* gene and was designated the Δ*purH* + *purH* strain. The Δ*purH* + *purH* strain was constructed as follows. The region encompassing the 1.5-kb *purH* gene and 500 bp upstream of the *purH* gene was PCR amplified using Qiagen Master Mix with *B. anthracis* Ames strain genomic DNA as the template. The gene fragment was then cloned into KpnI/PmeI restriction sites in the *E. coli* shuttle vector pEO3, yielding plasmid pEO3-*purH*. The plasmid was integrated into the chromosome of the mutant strain, upstream of the Ω-Kan-2 fragment, and cointegrate clones were selected based on kanamycin, erythromycin, and temperature (42°C) resistance. Clones that were found to be antibiotic resistant were screened for the presence of the cointegrate in the mutated genome by PCR analysis. The resulting genetically complemented (Δ*purH* + *purH*) mutant strain contained the Ω-Kan-2 fragment from the original mutant and a full-length, intact *purH* gene.

Second, Δ*purH* was complemented with a full-length, intact *purD* open reading frame and was designated the Δ*purH* + *purD* strain. The Δ*purH* + *purD* strain was constructed as follows. The 1.3-kb *purD* gene was PCR amplified from Ames genomic DNA using Qiagen Master Mix. Separately, the 500-bp upstream flanking region of the *purH* gene was PCR amplified from Ames genomic DNA. The 500-bp upstream *purH* fragment and the 1.3-kb *purD* gene were then cloned into KpnI/XbaI restriction sites, with a SmaI restriction site linking the two fragments, in the *E. coli* shuttle vector pEO3, giving plasmid pEO3-i.f.-*purD*. The *purD* gene was PCR amplified and cloned into the pEO3 vector with the *purH* upstream region in frame, so the resulting Δ*purH* + *purD* strain contained the *purD* open reading frame, in frame, in place of the *purH* gene. The pEO3-i.f.-*purD* plasmid was treated in the same manner as described above. The resulting genetically complemented (Δ*purH* + *purD*) mutant strain contained the Ω-Kan-2 fragment from the original mutant and a full-length, intact *purD* gene.

To genetically complement Δ*purD*, the same approach as for the Δ*purH* + *purH* strain was taken. The Δ*purD* + *purD* strain was constructed as follows. The region including the 1.3-kb *purD* gene and 500 bp upstream of the *purD* gene was PCR amplified from Ames genomic DNA using Qiagen Master Mix. The gene fragment was then cloned into KpnI/XbaI restriction sites in the *E. coli* shuttle vector pEO3, giving plasmid pEO3-*purD*. The resulting plasmid was treated in the same manner as described above. The genetically complemented (Δ*purD* + *purD*) mutant strain contained the Ω-Kan-2 fragment from the original mutant and a full-length, intact *purD* gene.

Verification of virulence factors in mutant strains. Retention of the pXO1 and pXO2 plasmids was assayed by PCR using primers specific for the *pagA* (15) and *capC* genes, respectively. Capsule production was verified in all strains by growth on Trypticase soy agar (TSA) plates containing bicarbonate. The plates were grown overnight at 37°C with 20% CO_2. To assay for the production of protective antigen (PA), all strains were grown in R-medium (60), with or without bicarbonate, supplemented with 5% fetal bovine serum. At various time points after inoculation, an aliquot was removed from each culture; the aliquot was centrifuged to pellet the cells; and the supernatant was removed. Western blotting of the supernatants from each sample was then performed using rabbit anti-PA antibodies (15).

***In vitro* growth phenotypes.** All growth curves were determined by measuring an increase in the optical density at 600 nm (OD_{600}) in rich LB medium or the minimal R-medium (60). Where indicated, the medium was supplemented with purines at a final concentration of 1 mM. To determine growth in R-medium, overnight cultures grown in LB medium were centrifuged, and the pellets were resuspended and washed four times with R-medium. The washed cells were then resuspended in a defined volume of R-medium to begin growth.

Virulence testing in the mouse and rabbit models. Mice were challenged intraperitoneally and intranasally with wild-type, *purH*::Kan, Δ*purH*, or Δ*purD* spores, as described previously (14, 16, 42). Rabbits were challenged subcutaneously with varying doses of wild-type or *purH*::Kan spores (71). The challenge doses delivered are given in the figure legends.

Virulence testing and *in vivo* fitness assay in the guinea pig model. Guinea pigs were challenged intramuscularly (7), intraperitoneally (22), or by aerosol exposure (40) with varying doses of wild-type, *purH*::Kan, Δ*purH*, or Δ*purD* spores. The challenge doses delivered are given in the figure legends.

The guinea pig *in vivo* fitness model was utilized as described previously (6, 13). Briefly, guinea pigs were challenged intramuscularly with an approximately equal mixture of wild-type Ames spores and mutant spores. Two days after challenge, moribund guinea pigs were euthanized, and their spleens were harvested and homogenized. The splenic bacterial loads were determined by plating the homogenates onto LB plates or LB plates with kanamycin to assess the relative ratio of wild-type bacteria to mutant bacteria recovered from each spleen.

Guinea pigs were also challenged intraperitoneally with wild-type Ames or *purH*::Kan bacilli. The bacilli were generated from spores that had been incubated in brain heart infusion (BHI) broth for approximately 2 h at 37°C, to give a final challenge dose of approximately 3×10^5 heat-sensitive CFU (~70% of which was single cells, while ~30% was chains consisting of two cells, as determined by microscopy). The bacilli were washed with phosphate-buffered saline (PBS) before the challenge to ensure that extracellular toxins were removed from the challenge material.

Guinea pigs were challenged intramuscularly with varying doses of Δ*purH* spores for determination of the 50% lethal dose (LD_{50}) and time to death (TTD) and were followed for 14 days. PA in the blood and edema in dead or moribund guinea pigs was assayed by Western blot analyses as described above. Cyclic AMP (cAMP) concentrations in the guinea pig edema were assayed using the direct cAMP determination kit from Sigma-Aldrich according to the manufacturer's specifications.

Histology. Samples for histopathology were immersion-fixed in 10% neutral buffered formalin for 30 days. Sections prepared for examination using light microscopy were embedded in paraffin, sectioned, and stained with hematoxylin and eosin (HE). Immunohistochemistry (IHC) was performed on sections using a monoclonal mouse antibody to *B. anthracis* polyglutamic acid capsule at 1:8,000 as a primary antibody and a peroxidase-labeled polymer (EnVision peroxidase kit; Dako Corp., Carpinteria, CA) as a secondary antibody. The slides were stained with a substrate-chromogen solution and were counterstained with hematoxylin. As previously described, malachite green staining was also performed to identify ungerminated spores (69).

Statistics and computer software. Survival rates were compared between treatment and control groups by Fisher exact tests with permutation adjustment for multiple comparisons. Kaplan-Meier product-limit estimation was used to construct survival curves and to compute mean survival times. Survival curves were compared between treatment and control groups by log rank tests with Hochberg adjustment for multiple comparisons. Mean TTD values for each treatment group were compared with those of the control group by *t* tests with permutation adjustment for multiple comparisons. The analyses described above were conducted using SAS, version 8.2 (SAS OnlineDoc, version 8, 2000; SAS Institute, Inc., Cary, NC). Biosynthetic pathway analysis was performed using the Kyoto Encyclopedia of Genes and Genomes (KEGG) database (http://www.genome.jp/kegg). Additional genome analysis and open reading frame determination were carried out using The SEED database (http://theseed.uchicago.edu/FIG/index.cgi). When relative bacterial counts (i.e., those recovered from spleens) were compared, statistical significance (P, <0.05) was determined by the two-tailed Student *t* test with GraphPad Prism software (GraphPad, San Diego, CA).

RESULTS

Identification and characterization of the *purH* gene. A Tn*10* transposon library of the Sterne strain of *B. anthracis* was screened for clones with altered phenotypes (13). Rescue cloning and sequencing identified a gene (BAS0285 in the Sterne strain; BA0298 in the Ames strain) encoding the bifunctional protein IMP cyclohydrolase/phosphoribosyl aminoimidazolecarboxamide formyltransferase (PurH). PurH catalyzes the final two steps in the biosynthesis of the purine IMP (Fig. 1A). In most bacteria, the genes encoding the proteins required for this pathway are maintained as a 12-gene operon (1, 19, 20, 24). The *purH* gene is the penultimate gene in the *pur* operon sequence (Fig. 1B), followed by *purD* (20, 24). Therefore, it is possible that a mutation in the *purH* gene results in a polar effect on *purD*. To evaluate the role that *de novo* purine biosynthesis plays in the virulence and pathogenesis of *B. anthracis*, *purH* mutant strains were assessed. While any mutation in the genes of the IMP biosynthetic pathway will likely cause complete disruption of *de novo* purine biosynthesis, the *purH* mutant strains were chosen because PurH is the final enzyme in the biosynthetic pathway, and it is encoded by the gene identified in our library screen.

A *purH* mutant strain (designated the *purH*::Kan strain) was created in the fully virulent Ames strain by inserting the Ω-Kan-2 cassette (57) into a unique BamHI restriction site (888 bp downstream of the ATG start codon) in the native *purH* gene. Since PurH is known to be a bifunctional enzyme, we also created a deletion mutation of the *purH* gene to ensure that a functional truncated protein was not possible (Δ*purH*). The Δ*purH* strain was constructed by replacing the *purH* gene with the Ω-Kan-2 cassette in the wild-type Ames strain, thereby removing the entire *purH* coding region. It should be noted that the insertion of the Ω-Kan-2 cassette into the *pur* operon potentially caused a polar effect on the *purD* gene; however, our goal was to determine the overall role of purine biosynthesis in *B. anthracis* virulence. Establishing an association between the lack of purine production and a particular gene or genetic mutation was not an objective. Both *purH* mutant strains of *B. anthracis* retained the two virulence plasmids, as determined by PCR analysis and functional assays. The mutant strains produced capsules, as determined by assays on bicarbonate plates (data not shown). In addition, the mutant and parental strains produced similar amounts of PA, as determined by immunoblotting (data not shown).

Growth of the *purH*::Kan and Δ*purH* strains and complementation of the growth phenotype. To determine the growth requirements and phenotype of the *purH*::Kan and Δ*purH* mutant strains, both wild-type Ames and *purH* mutant bacilli were grown in rich (LB) medium or minimal medium (R-medium). In rich medium, the *purH* mutants and the wild-type strain grew similarly (data not shown). In contrast, the *purH* mutant strains were unable to grow appreciably in minimal medium compared with the Ames parent strain (Fig. 2A). When R-medium was supplemented with inosine, to demonstrate the ability of *purH* mutants to scavenge the necessary nutrients, the *purH* mutant strains grew at approximately the same rate as the wild-type Ames strain (Fig. 2B). Adenosine was also sufficient to rescue the growth defect of the mutant strains (data not shown). As expected, these results suggested that PurH was required for *B. anthracis* purine biosynthesis.

The *purH* mutation was genetically complemented using two different approaches. First, the Δ*purH* strain was complemented with an intact *purH* gene and was designated the Δ*purH* + *purH* strain. To ensure that the phenotypes described here could not be attributed solely to a polar effect on the *purD* gene, the intact *purD* open reading frame was also used to genetically complement the Δ*purH* mutation. In this complementation, *purD* was integrated into the Δ*purH* genome in place of the *purH* gene. The cointegrate was designed in such a manner as to ensure that the *purD* open reading frame remained in frame with the native *pur* operon, with the *purD* start codon in the same position as the original *purH* start codon. Therefore, this strain, designated the Δ*purH* + *purD* strain, had no *purH* gene but contained an intact, in-frame *purD* gene uninterrupted by the presence of the Ω-Kan-2 fragment, in addition to the native *purD* gene located downstream of the Ω-Kan-2 fragment.

To determine the growth requirements and phenotype of

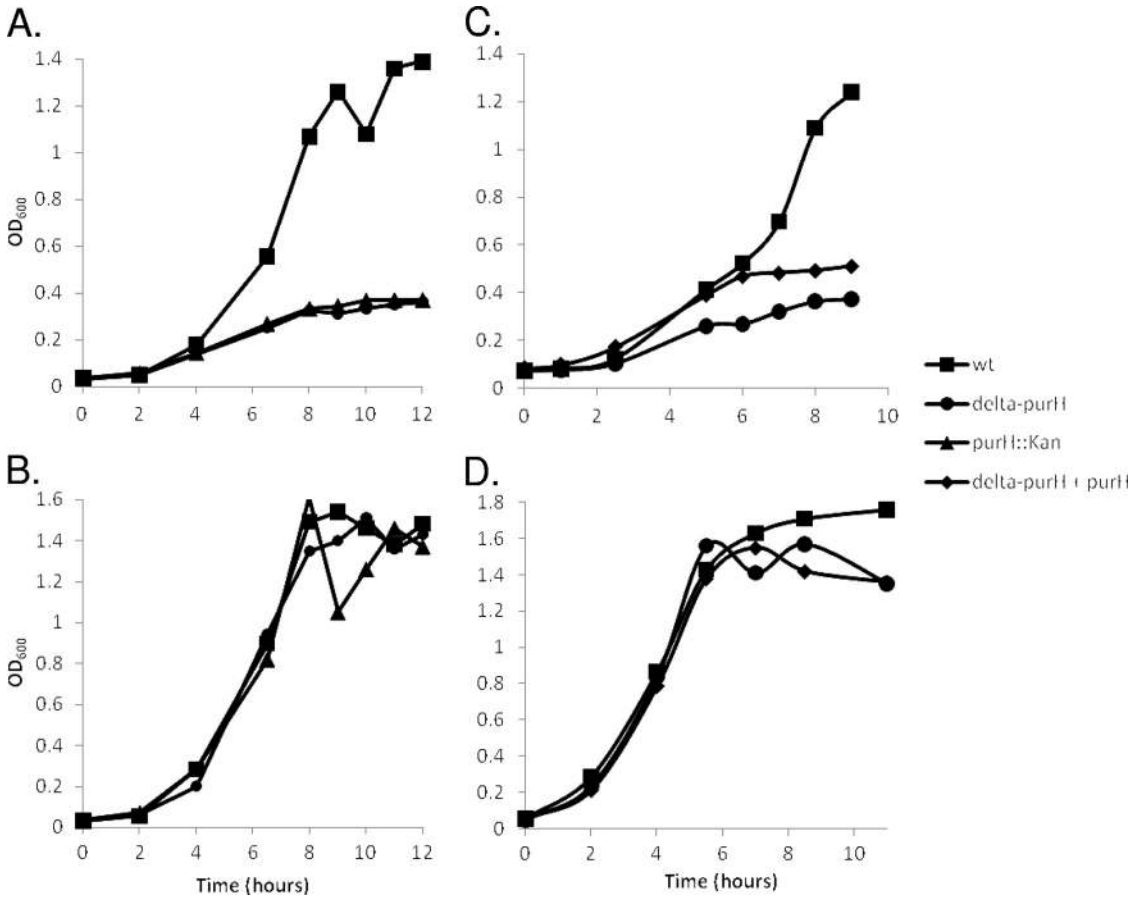

FIG. 2. Representative growth curves for the wild-type (wt), *purH*::Kan, Δ*purH*, and Δ*purH* + *purH* strains. The strains were grown in the minimal defined R-medium (A and C) or in R-medium supplemented with 1 mM inosine (B and D). These data represent the results of at least two experiments.

the genetically complemented mutant strains, wild-type Ames bacilli and Δ*purH*, Δ*purH* + *purH*, and Δ*purH* + *purD* mutant bacilli were grown in minimal R-medium. The Δ*purH* + *purH* strain was viable in R-medium, although it did not grow to the same level as the wild-type Ames strain during the first 10 h of culture growth (Fig. 2C). It should be noted that the Δ*purH* + *purH* strain grew to approximately the same OD_{600} as the wild-type Ames strain after an extended incubation period of 24 to 36 h, while the Δ*purH* strain never reached an OD_{600} approaching that of the wild-type Ames strain (data not shown). When R-medium was supplemented with inosine, the mutant and complemented strains grew at approximately the same rate as the wild-type Ames strain (Fig. 2D). The Δ*purH* + *purD* strain was unable to grow to any appreciable levels in R-medium compared to those of the Ames parent strain, even after an extended growth period of 24 to 36 h (data not shown). Therefore, while there is likely a polar effect on *purD* in the Δ*purH* mutant, the *in vitro* phenotype observed for the Δ*purH* strain is not associated solely with the effects on *purD*; rather, an intact *purH* gene is also required for complete growth. As expected, the addition of inosine to the growth medium was able to restore growth of the Δ*purH* + *purD* strain to wild-type levels (data not shown).

The partial complementation (lower rate of growth than that of the wild type) of the Δ*purH* + *purH* strain may be due to a polar effect on *purD*. RT-PCR analysis of the Δ*purH* mutant demonstrated that even in the absence of *purH*, detectable levels of *purD* transcript were present. Detectable levels of *purD* were also present in the Δ*purH* + *purH* strain. These data suggest that while a polar effect on *purD* is possible, it is not causing a complete loss of *purD* expression (Fig. 3). The RT-

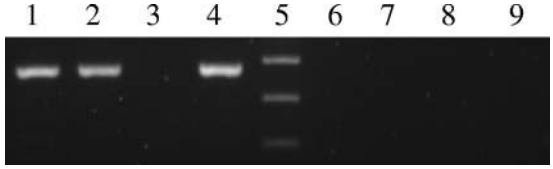

FIG. 3. Reverse transcription-PCR was performed on total RNA harvested from cultures of *B. anthracis*. The reactions used primers specific for an internal fragment of the *purD* gene (approximately 380 bp). Lane 1, wild-type RNA; lane 2, RNA collected from the Δ*purH* strain; lane 3, RNA collected from the Δ*purD* mutant strain; lane 4, RNA collected from the Δ*purH* + *purH* strain. Lane 5, 1 KB Plus ladder; bands shown, from bottom to top, are 200 bp, 300 bp, and 400 bp. Lanes 6 to 9, corresponding negative controls to confirm the absence of DNA from the RNA samples. Additionally, positive controls (not shown) were run using primers specific for the *pagA* gene as an internal control to ensure the quality of the harvested RNA.

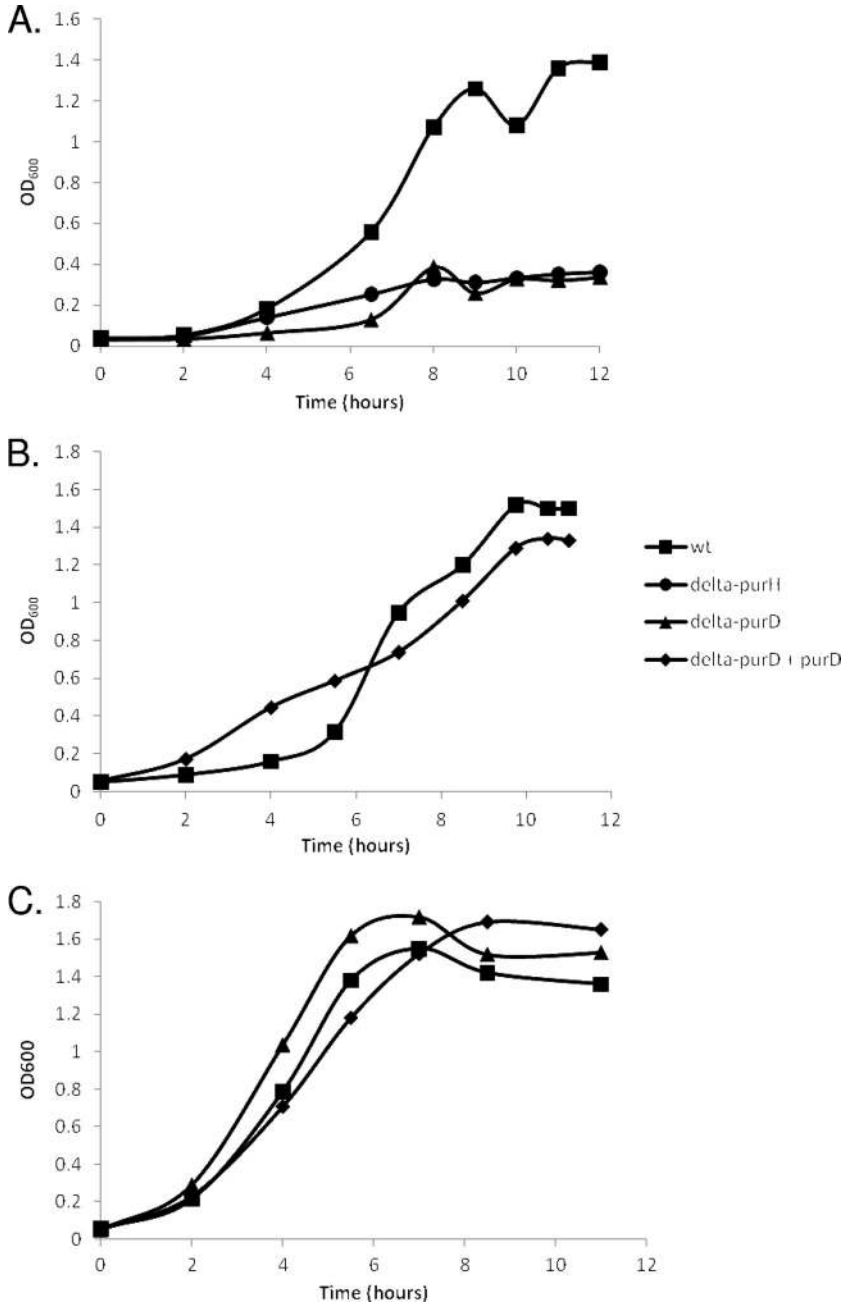

FIG. 4. Representative growth curves for the wild type (wt) and for the Δ*purH*, Δ*purD*, and Δ*purD* + *purD* mutant strains. The strains were grown in the minimal defined R-medium (A and B) or in R-medium supplemented with 1 mM inosine (C). These data are representative of at least two experiments.

PCR data corroborate the results observed for Δ*purH* + *purH* growth, in that the addition of an intact *purH* gene to the Δ*purH* mutant gives partial complementation, suggesting that *purD* is expressed to some level in the Δ*purH* mutant. While complete complementation of the Δ*purH* strain may have been accomplished by the construction of a strain harboring both wild-type *purH* and *purD* genes, we were unable to construct this strain, likely due to the double recombination of this complemented strain yielding a wild-type genotype. It should also be noted that it is unlikely that the observed Δ*purH* phenotype is due to a mutation elsewhere in the genome (outside the purine operon), since the growth phenotype was completely complemented by the addition of exogenous purines (Fig. 2).

To assess the role of PurD in purine biosynthesis, a Δ*purD* strain was constructed in the same manner as the Δ*purH* strain. The Δ*purD* strain exhibited the same *in vitro* phenotypes as the Δ*purH* strain, as expected (Fig. 4A and C). A genetically complemented Δ*purD* strain (Δ*purD* + *purD*) was also constructed. In R-medium, the Δ*purD* + *purD* strain grew at rates similar to those of the wild-type Ames strain (Fig. 4B). It should be noted

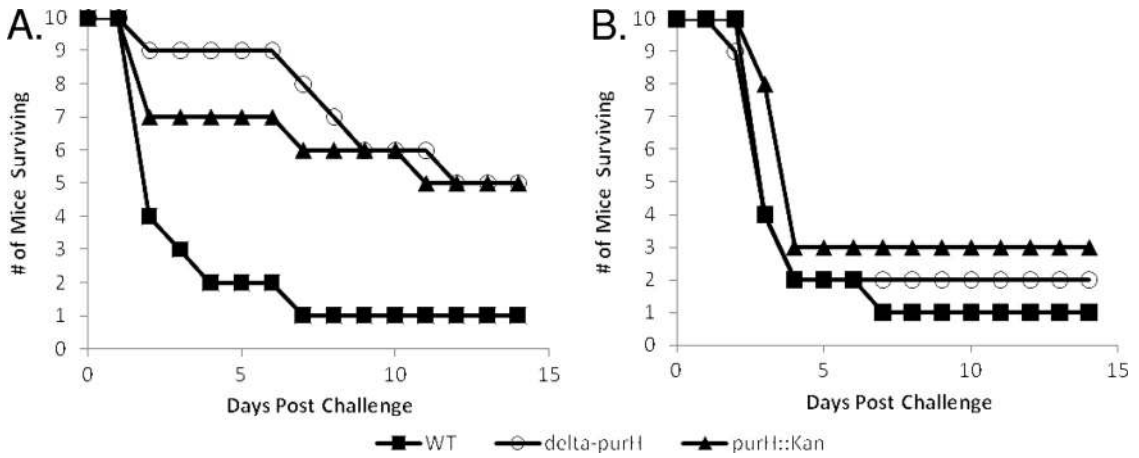

FIG. 5. Mouse intraperitoneal and intranasal challenges with wild-type (WT) Ames or *purH* mutant spores. (A) BALB/c mice were challenged intraperitoneally with approximately 3×10^3 wild-type Ames, 3×10^3 *purH*::Kan (*P*, 0.09 for the survival curve and 0.6 for the percentage of mice surviving), or 2.3×10^3 Δ*purH* (*P*, 0.023 for the survival curve and 0.6 for the percentage of mice surviving) spores. (B) BALB/c mice were challenged intranasally with approximately 3.2×10^6 wild-type Ames, *purH*::Kan, or Δ*purH* spores delivered in 50 μl. These data represent at least two experiments.

that while purine biosynthesis and thiamine biosynthesis are linked through a common intermediate, all the mutants discussed here were able to grow in media lacking thiamine (data not shown). The results generated by *in vitro* analysis suggest that both PurH and PurD are required for growth in R-medium lacking purines and that both can be rescued by the addition of exogenous purines. This emphasizes the point that the lack of growth of the Δ*purH* and Δ*purD* strains *in vitro* is due to a lack of *de novo* purine biosynthesis.

***In vivo* determination of the virulence of the *purH* mutant in small-animal models. (i) Mice and rabbits.** BALB/c mice were challenged either intraperitoneally (Fig. 5A) or intranasally (Fig. 5B) with wild-type Ames or *purH* mutant strain spores. While significant differences in the survival curve (but not in the percentage of animals surviving) were noted when the Δ*purH* spores were administered intraperitoneally, no statistically significant differences were observed when the *purH* mutant spores were administered intranasally (Fig. 5B).

A staircase experiment to evaluate the virulence of the *purH*::Kan mutant in rabbits was performed. Six rabbits were each sequentially given a single subcutaneous challenge dose of the *purH*::Kan spores at six concentrations increasing from 1.6×10^2 to 1.6×10^7. These data were used to calculate a Dixon staircase LD_{50} (17) of 381 spores with a mean TTD of approximately 3 days postchallenge. The LD_{50} reported previously for spores of the Ames strain injected subcutaneously into rabbits is approximately 1.6×10^3 spores, and the mean TTD was reported to be approximately 3 days depending upon the challenge dose administered (71). Since the LD_{50} values were calculated using different methods (probit versus Dixon staircase), and since no confidence intervals were reported for the published value, the two values cannot statistically be compared. However, we can conclude that no attenuation was observed when *purH* mutant spores were given subcutaneously to rabbits. It should be noted that initial studies were performed with the *purH*::Kan mutant. The Δ*purH* mutant strain was then constructed to ensure that there were no truncated PurH peptides that could retain partial activity *in vivo*. There were no significant differences between the *purH*::Kan and Δ*purH* strains in either mouse or guinea pig models. Thus, we believed that these data did not warrant a second iteration of the rabbit experiment, since there is no evidence that the Δ*purH* strain would be any more or less virulent than the *purH*::Kan strain.

(ii) Guinea pigs. To determine the relative virulence and bacterial fitness of the *purH* mutant strains, a competitive assay was performed using the guinea pig intramuscular model of infection (6, 13). No *purH* mutant bacteria were recovered from the guinea pig spleens examined (approximate limit of detection, 10 CFU/g of spleen) (Fig. 6A). Survival experiments further indicated that the spores of the *purH* mutants were significantly attenuated when injected intramuscularly into guinea pigs. Guinea pigs challenged intramuscularly with approximately 1×10^3 *purH*::Kan or Δ*purH* spores survived and showed no signs of illness or distress. In contrast, guinea pigs infected with approximately 1×10^3 Ames strain spores were found dead or were euthanized if moribund within 48 h after infection (Fig. 6B).

To ensure that this attenuation was not specific to the challenge route, guinea pigs were also challenged intraperitoneally with spores of the Ames or Δ*purH* strain. Whereas 20% of the guinea pigs challenged with Ames spores survived the infection, 100% of the guinea pigs challenged with Δ*purH* spores survived (Fig. 6C). Additionally, guinea pigs were exposed to aerosolized *purH*::Kan spores. The guinea pigs inhaled approximately 9.5×10^6 *purH*::Kan spores (approximately 250 Ames wild-type LD_{50} equivalents [31]), and again, 100% ($n = 4$) of the animals survived the infection, showing no signs of illness or distress (data not shown). These data demonstrate a significant attenuation associated with *purH* mutant strains of *B. anthracis* in guinea pigs, while little or no attenuation was observed in the mouse and rabbit models.

We hypothesized multiple causes for the discrepancies between animal models. These studies suggest that the distribution or availability of purines in guinea pigs must be significantly different from that in mice or rabbits. There are several

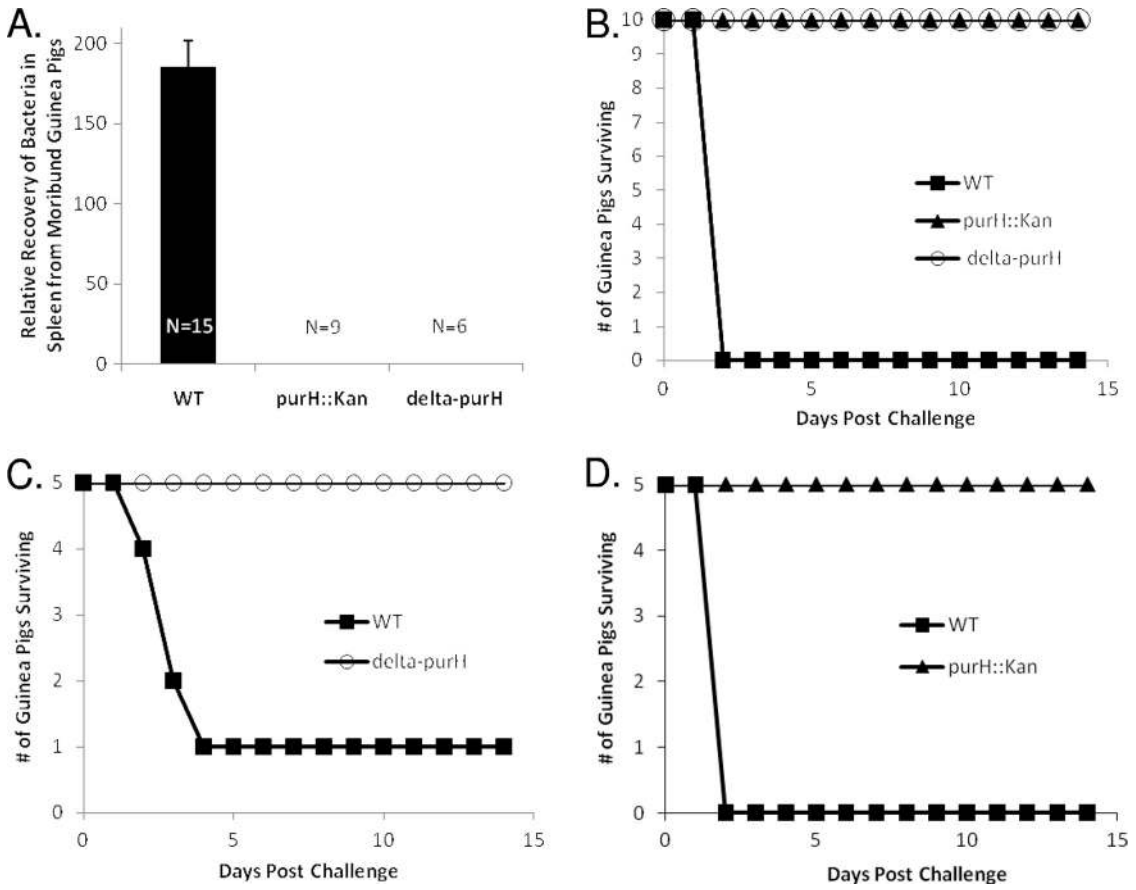

FIG. 6. Guinea pig challenges with wild-type (WT) Ames or *purH* mutant strains. (A) Competitive index generated from the guinea pig assay for comparison of the *in vivo* fitness of *purH* mutant strains to that of the wild-type Ames strain ($P < 0.0001$). Guinea pigs were challenged intramuscularly with approximately 1×10^3 spores consisting of approximately equal ratios of wild-type and mutant spores. (B) Guinea pigs were challenged intramuscularly with approximately 1×10^3 wild-type Ames, *purH*::Kan, or Δ*purH* spores (P, <0.0001 for both the percentage of animals surviving and the survival curve), (C) Guinea pigs were challenged intraperitoneally with approximately 4×10^4 wild-type Ames or Δ*purH* spores (P, 0.025 for the percentage of animals surviving and 0.04 for the survival curve). (D) Guinea pigs were challenged intraperitoneally with approximately 1.6×10^5 CFU of wild-type Ames or *purH*::Kan bacilli (P, 0.008 for the percentage of animals surviving and 0.003 for the survival curve).

scenarios that could also contribute to attenuated virulence in the guinea pig. One possibility is that *purH* mutant spores germinate slowly or incompletely in the guinea pig, making them unable to cause systemic disease. Additionally, we hypothesized that the vegetative bacilli of *purH*-negative strains may be unable to grow efficiently and to produce the exotoxins required for disease progression in guinea pigs due to a lack of available purine nucleosides.

To assess a role for purine deficiency in the attenuation of the *B. anthracis purH* mutants in guinea pigs, we challenged guinea pigs intramuscularly with approximately 1×10^3 *purH*::Kan mutant spores in a suspension containing either 1 mM inosine or 1 mM adenosine. Neither the addition of inosine nor that of adenosine had any effect on *purH* spore infectivity; 100% of the challenged animals survived (data not shown). To further assess the apparent avirulence of the *purH* mutant in guinea pigs, a septicemic model of infection was utilized. Guinea pigs were challenged intraperitoneally with bacilli of the wild-type Ames or *purH*::Kan strain. All guinea pigs challenged with wild-type Ames bacilli succumbed to disease within 48 h. In contrast, the guinea pigs challenged with the *purH*::Kan bacilli survived and showed no signs of illness or distress (Fig. 6D).

To determine if a mutation in the *purH* gene results in a strain that is completely avirulent in guinea pigs, an intramuscular LD_{50} experiment was performed (Fig. 7). While these data did not permit the determination of a statistically reliable intramuscular LD_{50} for guinea pigs, the value is greater than 10^6 spores for the Δ*purH* mutant strain. The intramuscular LD_{50} of the wild-type Ames strain is reportedly 100 spores (32), but recent work has suggested that the LD_{50} may be significantly lower (A. M. Friedlander, personal communication). Statistically significant differences in mean TTD values between animals infected with Δ*purH* mutant versus wild-type spores were also observed. Whereas guinea pigs receiving approximately 1×10^3 wild-type Ames spores had a mean TTD of 2 days, guinea pigs succumbing to a challenge with 1×10^7 spores of the Δ*purH* mutant had a mean TTD of 7.4 ± 2.07 days (P, 0.002); nonsurvivors challenged with 1×10^6 spores had a mean TTD of 10.5 ± 2.12 days (P, 0.0006). These data are particularly noteworthy when one considers the disparate doses required for lethality.

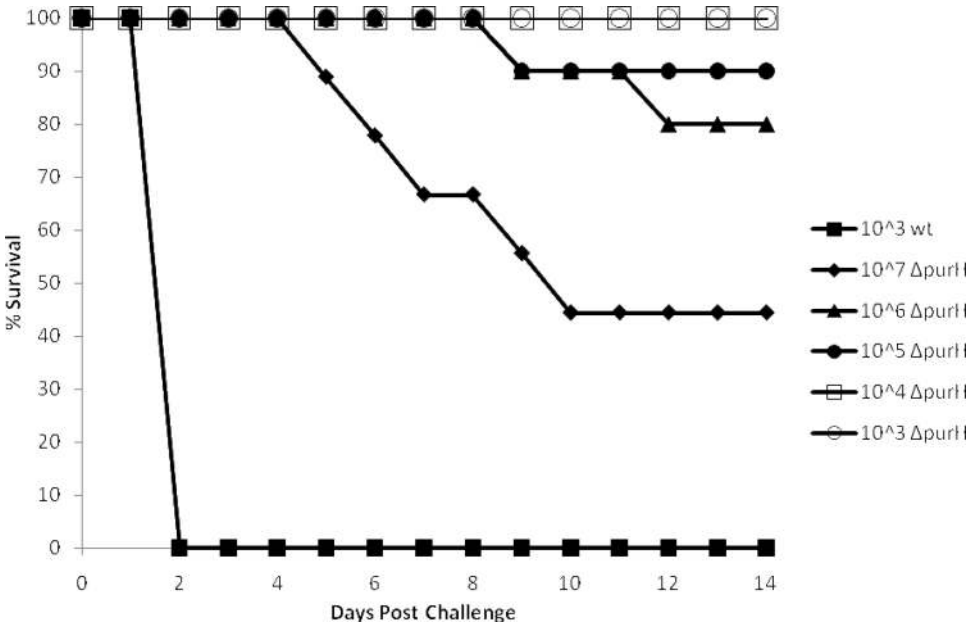

FIG. 7. LD_{50} results for Δ*purH* spores injected intramuscularly into guinea pigs.

Samples from guinea pigs terminally infected with Δ*purH* spores were collected for bacterial culture and histological analyses (Fig. 8). After intramuscular challenge with high doses of Δ*purH* spores, moribund guinea pigs had difficulty moving and exhibited striking edema accompanied by extension of the dorsal skin. At necropsy, there was marked thickening of the subcutaneous tissues and intermuscular fascial planes with a thick, amber-colored gelatinous material (Fig. 8A). This material was collected and cultured, and the liquid phase of the gelatinous edema was assayed both for cAMP levels (presumably due to edema toxin) and for the PA component of the anthrax exotoxins. The portion of edema not contaminated with blood was culture negative for *B. anthracis* but showed increased levels of cAMP (data not shown). In addition, PA was detected by immunoblotting in the fluid phase of the edema and, to a lesser extent, in the sera, indicating the presence of anthrax toxin components (data not shown).

Guinea pigs infected with Δ*purH* spores had significantly lower (*P*, 0.006) splenic bacterial burdens than guinea pigs challenged with wild-type Ames spores, even though the initial dose of Ames spores was 3 to 4 orders of magnitude lower than the Δ*purH* spore dose (Table 3). Blood cultures were compared for several of the guinea pigs, and the bacterial loads in Δ*purH* mutant-challenged animals ($n = 3$) were significantly lower than those in guinea pigs infected with Ames spores (*P*, 0.02) (Table 4).

Histopathological analyses of guinea pig specimens. Samples of spleens and skeletal muscle were collected from the sites of injection of guinea pigs lethally infected with high doses of Δ*purH* spores. Immunohistochemistry (IHC) was performed on select sections of spleen and skeletal muscle using a mouse anti-capsule antibody. Myriad bacilli were present in histologic sections of skeletal muscle that were also strongly positive by IHC for *B. anthracis* capsule antigen. These analyses clearly demonstrated that the Δ*purH* spores were capable of germinating and forming encapsulated vegetative cells within the muscle tissue at the site of injection (Fig. 8B and C). In addition, histologic changes in skeletal muscle included degeneration and necrosis of skeletal muscle fibers, infiltration of moderate numbers of inflammatory cells (primarily polymorphonuclear cells), and marked edema (Fig. 8B and C). Bacilli or spores could not be readily identified in histologic sections of spleen, but low levels of bacteria were detected by plate counts of spleen homogenates (Table 3). Thus, the bacteria present were below the limit of microscopic detection.

There was lymphocytolysis with generalized lymphoid depletion within the white pulp (lymphocyte areas located within the spleen) of some of the animals (Fig. 8D and E). These changes have been documented frequently in animal anthrax models and are considered to be key features of this disease (18, 27, 64, 65) or of intoxication with anthrax toxins alone (23, 39). These data suggest that the spores were being retained at the site of injection, germinating, and forming vegetative (toxin-producing) bacilli. We propose that when sufficient numbers of *purH* vegetative cells are present, the anthrax toxins produced eventually reach lethal systemic levels.

Genetic complementation of the *purH* strain *in vivo*. When guinea pigs were challenged intramuscularly with the Δ*purH* + *purH* strain, 80% of them succumbed to infection (Fig. 9). These results suggest partial complementation of the Δ*purH* phenotype. While there were no statistical differences in the percentage of survival between animals challenged with the complemented strain and wild-type Ames-infected animals, the mean TTD was significantly extended for the former group. The extended mean TTD correlates well with the delayed growth of the Δ*purH* + *purH* strain *in vitro*. When guinea pigs were challenged intramuscularly with the Δ*purH* + *purD* strain, 20% of them succumbed to infection (Fig. 9). These results suggest no significant complementation of the Δ*purH* pheno-

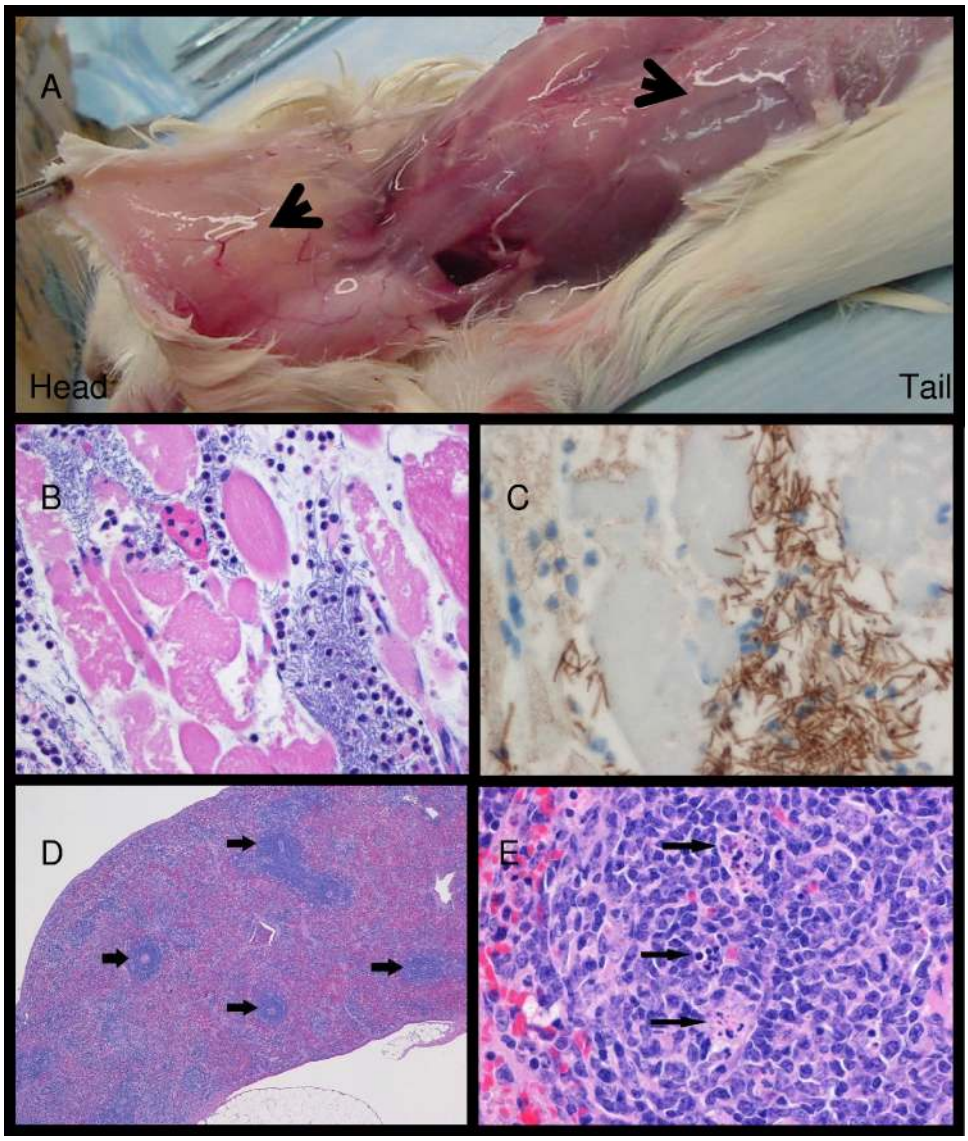

FIG. 8. Guinea pigs infected with the Δ*purH* strain of *B. anthracis*. Moribund guinea pigs appeared to be "swollen." (A) Marked subcutaneous and fascial plane edema. Note the thickened and glistening (marked edema) subcutaneous tissues (arrows). (B) Skeletal muscle of a guinea pig infected with the Δ*purH* strain of *B. anthracis*. There is skeletal muscle degeneration and necrosis characterized by variation in the size and shape of skeletal muscle fibers, loss of cross-striations, and fractured and vacuolated sarcoplasm (cytoplasm). The connective tissue between muscle fibers is markedly expanded by myriad bacilli, polymorphonuclear inflammatory cells, and clear space (edema). HE was used for staining; magnification, ×20. (C) Skeletal muscle, at the injection site, of a guinea pig infected with the Δ*purH* strain of *B. anthracis*. There are myriad strongly positive bacilli within the connective tissue between muscle fibers and invading skeletal muscle fibers. The strong IHC positivity suggests that the bacilli in the muscle produced robust capsules. Immunohistochemistry was carried out for the *B. anthracis* capsule antigen, with a hematoxylin counterstain; magnification, ×60. (D) Spleen of a guinea pig infected with the Δ*purH* strain of *B. anthracis*. There is diffuse paucity of splenic white pulp. There are scattered normal periarteriolar lymphoid sheaths (arrows). HE was used for staining; magnification, ×4. (E) Spleen of a guinea pig infected with the Δ*purH* strain of *B. anthracis*. Lymphocytolysis (arrows) is evident within the germinal center of a splenic corpuscle. HE was used for staining; magnification, ×40.

TABLE 3. Bacterial loads determined in the spleens of guinea pigs infected intramuscularly with either wild-type Ames or Δ*purH* spores

Challenge strain	Challenge dose	Bacterial load (CFU/g)	No. of animals	% Recovery relative to challenge dose	*P*
Ames wt[a]	1×10^3	3.3×10^9	3	3.3×10^8	0.006
Δ*purH* strain	1×10^7	4.20×10^5	5	0.42	

[a] wt, wild type.

type by the addition of *purD*. A Δ*purD* strain, constructed in the same manner as the Δ*purH* strain, exhibited the same *in vivo* phenotypes as the Δ*purH* strain (data not shown). Additionally, the Δ*purD* strain was genetically complemented with an intact *purD* gene, and the complemented strain was designated the Δ*purD* + *purD* strain. Guinea pigs challenged intramuscularly with the Δ*purD* + *purD* strain all succumbed to infection at a rate statistically similar to that for guinea pigs challenged with wild-type Ames spores (Fig. 9). The results

TABLE 4. Bacterial loads determined in the blood of guinea pigs infected intramuscularly with either wild-type Ames or Δ*purH* spores

Challenge strain	Challenge dose	Bacterial load (CFU/ml)	No. of animals	% Recovery relative to challenge dose	*P*
Ames wt[a]	1×10^3	9.2×10^8	3	9.2×10^7	0.02
Δ*purH* strain	$\geq 1 \times 10^6$	3.4×10^3	3	0.34	

[a] wt, wild type.

generated by *in vivo* analysis suggest that both PurH and PurD are required for full virulence in guinea pigs. This, again, emphasizes the point that the lack of virulence of the Δ*purH* and Δ*purD* strains in guinea pigs is due to a lack of *de novo* purine biosynthesis.

DISCUSSION

To our knowledge, this is the first example of a host-specific nutrient requirement associated with a mutation in *B. anthracis*. An intact purine biosynthetic pathway, in particular the pathway producing IMP, appears to be necessary for complete virulence in a guinea pig model of infection. The purine biosynthetic requirement for virulence in murine and rabbit models of infection appears to be less stringent, in that IMP biosynthetic mutants (mutants of any enzyme prior to PurH in the biosynthetic pathway) are either fully virulent or only slightly attenuated. A modest, yet statistically significant, difference (*P*, 0.023) was noted between the survival curve of mice challenged intraperitoneally with the Δ*purH* strain and that of mice challenged with the wild-type strain. However, it should be noted that there were no statistically significant differences between the *purH*::Kan strain and the wild type and no significant differences from the wild type in the percentage of survival for either strain. Nevertheless, there was some evidence of a trend toward slight attenuation in the mouse intraperitoneal model of infection (Fig. 5A), but not in a mouse intranasal model (Fig. 5B). We hypothesize that this could be due to differences in purine availability between the peritoneum and the lungs/mediastinal areas.

Several instances of such host-dependent variations are present in the bacterial pathogen *Y. pestis*. Burrows and Gillett demonstrated that a lack of available asparagine resulted in guinea pig resistance to certain strains of *Y. pestis* (9). Meyer and colleagues also demonstrated that while an attenuated strain of *Y. pestis* was less virulent in guinea pigs, certain species of nonhuman primates developed a lethal infection (51). Oyston and coworkers demonstrated that a *Y. pestis aroA* mutant (an aromatic amino acid auxotroph) retained virulence in mice but was attenuated in guinea pigs (55). In contrast, aromatic-compound-dependent *B. anthracis* Sterne strain mutants are attenuated in both guinea pigs and mice (33).

The lack of purine biosynthetic enzymes has various effects on intrinsic bacterial virulence depending on the pathogen, the susceptibility of the host, and the nature of the mutation in the biosynthetic pathway. A recent report suggested that a mutation in the *purE* gene significantly attenuated the Sterne strain of *B. anthracis* in a septicemic model of infection, but a mutation in the *purK* gene did not (61). This study contradicts previous reports that mutations in the purine biosynthetic pathway before the production of IMP have no effect on virulence in a murine model of infection. This discrepancy be-

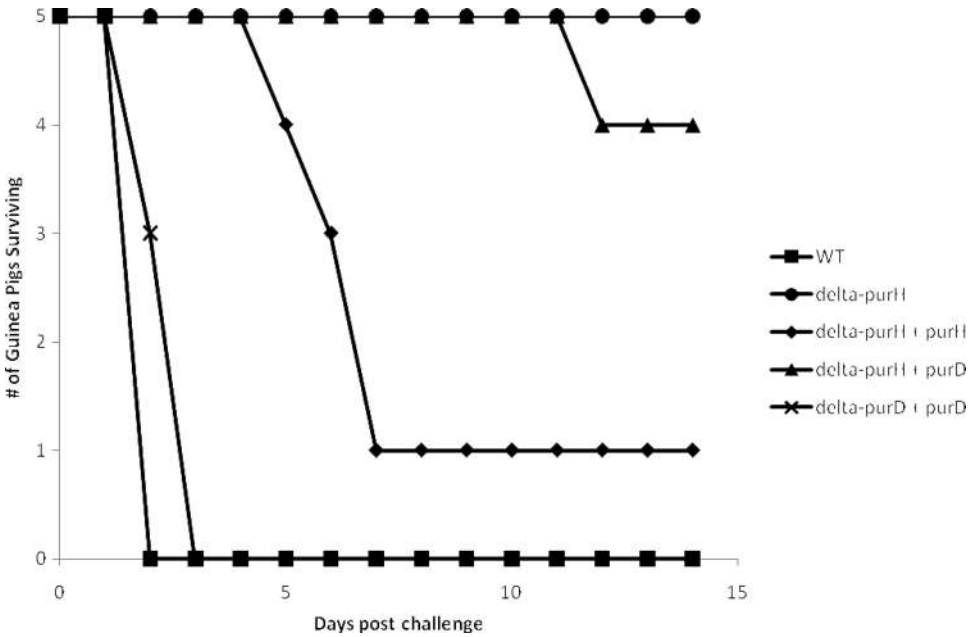

FIG. 9. Guinea pig challenges with wild-type (WT) Ames or complemented mutant strains. Guinea pigs were challenged intramuscularly with approximately 1×10^3 Ames, Δ*purH* (*P*, 0.017 for the percentage of guinea pigs surviving and 0.0240 for the survival curve compared with the WT), Δ*purH* + *purH* (*P*, 1 for the percentage of guinea pigs surviving, 0.024 for the survival curve, and <0.0001 for TTD compared with the WT), Δ*purH* + *purD* (*P*, 1 for the percentage of guinea pigs surviving and 0.3 for the survival curve compared with those for the Δ*purH* mutant), or Δ*purD* + *purD* (*P*, ≥0.05 for all tests conducted compared with the WT) spores.

tween the previous *B. anthracis* studies may be due to differences in *B. anthracis* strains (a fully virulent strain versus the attenuated Sterne strain used in the *purE* experiments), administration of bacilli in the septicemic model versus a spore challenge, and the use of mice that differ genetically. It has been shown previously that a defect in the biosynthesis of the purine nucleotides IMP and GMP had no effect on the virulence of *B. anthracis* in a mouse model, while mutations affecting the pathway converting IMP to AMP resulted in a significant attenuation of virulence in mice (30). Interestingly, a similar result has been reported for *Y. pestis*. Mutations in the purine biosynthetic pathway of *Y. pestis* occurring before the biosynthesis of IMP resulted in only an approximately 100-fold increase in the LD_{50} in mice, while mutations in the pathway between IMP and GMP showed a significantly higher degree of attenuation, resulting in a 10^7-fold increase in the LD_{50} in mice and a 10^8-fold increase in the LD_{50} in guinea pigs. No *Y. pestis* mutants with mutations in the pathway from IMP to AMP were isolated (8). A *purH* mutant of *Listeria monocytogenes* showed no change in virulence in a murine model of infection utilizing C3H mice, and a similar disruption in adenine production caused a 1.5-$\log_{10}$-fold increase in the LD_{50} of *L. monocytogenes* in BALB/c mice (38, 43). Interestingly, the plant pathogen *Xanthomonas oryzae* pv. *oryzae* was shown to require the PurH protein when infecting its natural host (rice plants) but not an alternate host (tomato plants) (12).

Our results presented here agree with the previous characterization of the fully virulent *B. anthracis* murine model in that mutations in genes involved in the biosynthesis of IMP have very little effect on virulence in mice (30) or rabbits; however, we observed a significant attenuation in virulence in the guinea pig model. This is the first example of a significant attenuation in virulence, albeit host specific, resulting from a genetic mutation disrupting the pathway prior to the production of IMP in a fully virulent *B. anthracis* strain. These studies emphasize the complexity of bacterium-host interactions and, in some cases, host specificity.

Our data demonstrate that the purine biosynthetic pathway, particularly the IMP biosynthetic pathway, of *B. anthracis* is required for full virulence in guinea pigs. We hypothesize that there is an inherent difference between the mechanism(s) used by guinea pigs to sequester or utilize purines and those of mice or rabbits. Importantly, IMP does not accumulate in the cell; rather, it is quickly converted to AMP and GMP in two enzymatic steps each. Therefore, the ultimate effect on the bacterial cell is due to a lack of AMP and GMP, not of inosine or IMP. Hence, a mutation in the *purH* gene should be rescued by the presence of a variety of purines in the growth medium or surrounding host tissue. Indeed, we showed that both inosine and adenosine complement the *in vitro* growth phenotype in the *purH* mutant strains. This suggests that these purines are not as readily available in guinea pigs as they may be in mice or rabbits. We hypothesize that in mice and rabbits, the mutant strains transport purines into the cells via purine nucleoside transporters. The salvaged purines are then converted into other purines via the available biosynthetic enzymes. The purine salvage pathways were not disrupted in the *purH* mutant strains; therefore, the lack of virulence and growth by the *purH* mutants in the guinea pig suggests that purines are not available at levels sufficient to promote bacterial growth. Injection of mutant strains into the guinea pig concomitantly with exogenous purines was unable to rescue the mutation (data not shown). This was most likely due to the low concentration of purines utilized and the short half-life of purines in animal models (5, 30, 58, 62). It is worth noting that while the IMP biosynthetic pathway was analyzed using *purH* and, in some cases, *purD* mutant strains, a mutation in any IMP biosynthetic gene (Fig. 1) should result in similar phenotypes based on the fact that the phenotypes are due to the lack of *de novo* purine biosynthesis.

Past research has highlighted physiological differences between purine metabolism in guinea pigs and that in other rodents. The concentration of adenosine is lower in the heart muscle tissue of guinea pigs than in those of rats and mice (28). While these findings highlight only one tissue, the possibility exists that the ratios of the levels of available purines in other tissues are similar. Additionally, significant differences were associated with purine transport into erythrocytes between guinea pigs and mice, rabbits, and other animals. It was suggested in this case that the differences in nucleoside transport in guinea pig erythrocytes were due to a difference in the number of nucleoside receptors present on the cell surface, resulting in a lower degree of nucleoside transport (34). These differences do not necessarily explain our observations, but they demonstrate a precedent for physiological differences in guinea pigs.

Although an inherent difference in the availability of purines in the body of a guinea pig is a plausible explanation for the differences in virulence between the wild-type Ames strain and the *purH* mutants, other possibilities do exist. As noted previously, *B. anthracis* mutants lacking an intact AMP biosynthetic pathway were avirulent in mice (30). The mutation could not be rescued even by injecting large amounts of exogenous adenine with the mutant strain. Ivánovics et al. suggested that an unknown virulence factor associated with AMP biosynthesis is required for infection in mice (30). This may also hold true for a purine biosynthetic mutant in guinea pigs. The lack of purine production may disrupt the production of an unidentified virulence factor required in guinea pigs. The capsule is an example of a virulence factor whose impact differs among different animal models for *B. anthracis* infection. For instance, it has been shown that some inbred strains of mice are relatively susceptible to infection with the unencapsulated *B. anthracis* Sterne strain, while other strains are significantly more resistant to infection (4, 66–70). Additionally, the LD_{50} of the *B. anthracis* Sterne strain in guinea pigs is reportedly 10^6 spores (11), demonstrating that capsule-negative strains are severely attenuated in guinea pigs. Toxin and capsule production were not affected in any appreciable manner in our *purH* mutant strains. Therefore, it is possible that the attenuated virulence of a *B. anthracis purH* mutant in guinea pigs is due to decreased production of an undefined virulence determinant and/or the lack of available host purines.

ACKNOWLEDGMENTS

We thank Diana Fisher for expert statistical analyses and Brad Stiles for critical reading of the manuscript.

The research described here was sponsored by the Defense Threat Reduction Agency JSTO-CBD as 02-4-5C-023 (to S.W.)/Medical Research/Material Command Research Plan.

The opinions, interpretations, conclusions, and recommendations presented here are those of the authors and are not necessarily endorsed by the U.S. Army.

Research was conducted in compliance with the Animal Welfare Act and other federal statutes and regulations relating to animals and experiments involving animals. The research adhered to the principles set forth in the *Guide for the Care and Use of Laboratory Animals* (National Research Council, 1996). The facility where this research was conducted is fully accredited by the Association for Assessment and Accreditation of Laboratory Animal Care International.

REFERENCES

1. **Aiba, A., and K. Mizobuchi.** 1989. Nucleotide sequence analysis of genes *purH* and *purD* involved in the de novo purine nucleotide biosynthesis of *Escherichia coli*. J. Biol. Chem. **264:**21239–21246.
2. **Allen, S., J. L. Zilles, and D. M. Downs.** 2002. Metabolic flux in both the purine mononucleotide and histidine biosynthetic pathways can influence synthesis of the hydroxymethyl pyrimidine moiety of thiamine in *Salmonella enterica*. J. Bacteriol. **184:**6130–6137.
3. **Beaman, T. C., A. D. Hitchins, K. Ochi, N. Vasantha, T. Endo, and E. Freese.** 1983. Specificity and control of uptake of purines and other compounds in *Bacillus subtilis*. J. Bacteriol. **156:**1107–1117.
4. **Beedham, R. J., P. C. Turnbull, and E. D. Williamson.** 2001. Passive transfer of protection against *Bacillus anthracis* infection in a murine model. Vaccine **19:**4409–4416.
5. **Bennett, E. L.** 1953. Incorporation of adenine into nucleotides and nucleic acids of C57 mice. Biochim. Biophys. Acta **11:**487–496.
6. **Bozue, J., C. K. Cote, K. L. Moody, and S. L. Welkos.** 2007. Fully virulent *Bacillus anthracis* does not require the immunodominant protein, BclA, for pathogenesis. Infect. Immun. **75:**508–511.
7. **Bozue, J. A., N. Parthasarathy, L. R. Phillips, C. K. Cote, P. F. Fellows, I. Mendelson, A. Shafferman, and A. M. Friedlander.** 2005. Construction of a rhamnose mutation in *Bacillus anthracis* affects adherence to macrophages but not virulence in guinea pigs. Microb. Pathog. **38:**1–12.
8. **Brubaker, R. R.** 1970. Interconversion of purine mononucleotides in *Pasteurella pestis*. Infect. Immun. **1:**446–454.
9. **Burrows, T. W., and W. A. Gillett.** 1971. Host specificity of Brazilian strains of *Pasteurella pestis*. Nature **229:**51–52.
10. **Carnrot, C., L. Wang, D. Topalis, and S. Eriksson.** 2008. Mechanisms of substrate selectivity for *Bacillus anthracis* thymidylate kinase. Protein Sci. **17:**1486–1493.
11. **Cataldi, A., M. Mock, and L. Bentancor.** 2000. Characterization of *Bacillus anthracis* strains used for vaccination. J. Appl. Microbiol. **88:**648–654.
12. **Chatterjee, S., and R. V. Sonti.** 2005. Virulence deficiency caused by a transposon insertion in the *purH* gene of *Xanthomonas oryzae* pv. *oryzae.* Can. J. Microbiol. **51:**575–581.
13. **Cote, C. K., J. Bozue, K. L. Moody, T. L. DiMezzo, C. E. Chapman, and S. L. Welkos.** 2008. Analysis of a novel spore antigen in *Bacillus anthracis* that contributes to spore opsonization. Microbiology **154:**619–632.
14. **Cote, C. K., J. Bozue, N. Twenhafel, and S. L. Welkos.** 2009. Effects of altering the germination potential of *Bacillus anthracis* spores by exogenous means in a mouse model. J. Med. Microbiol. **58:**816–825.
15. **Cote, C. K., C. A. Rossi, A. S. Kang, P. R. Morrow, J. S. Lee, and S. L. Welkos.** 2005. The detection of protective antigen (PA) associated with spores of *Bacillus anthracis* and the effects of anti-PA antibodies on spore germination and macrophage interactions. Microb. Pathog. **38:**209–225.
16. **Cote, C. K., N. van Rooijen, and S. L. Welkos.** 2006. The roles of macrophages and neutrophils in the early host response to *Bacillus anthracis* spores using a mouse model of infection. Infect. Immun. **74:**469–480.
17. **Dixon, W. J.** 1965. The up-and-down method for small samples. J. Am. Stat. Assn. **60:**967–978.
18. **Duong, S., L. Chiaraviglio, and J. E. Kirby.** 2006. Histopathology in a murine model of anthrax. Int. J. Exp. Pathol. **87:**131–137.
19. **Ebbole, D. J., and H. Zalkin.** 1989. *Bacillus subtilis pur* operon expression and regulation. J. Bacteriol. **171:**2136–2141.
20. **Ebbole, D. J., and H. Zalkin.** 1987. Cloning and characterization of a 12-gene cluster from *Bacillus subtilis* encoding nine enzymes for de novo purine nucleotide synthesis. J. Biol. Chem. **262:**8274–8287.
21. **Endo, T., B. Uratani, and E. Freese.** 1983. Purine salvage pathways of *Bacillus subtilis* and effect of guanine on growth of GMP reductase mutants. J. Bacteriol. **155:**169–179.
22. **Fellows, P. F., M. K. Linscott, B. E. Ivins, M. L. Pitt, C. A. Rossi, P. H. Gibbs, and A. M. Friedlander.** 2001. Efficacy of a human anthrax vaccine in guinea pigs, rabbits, and rhesus macaques against challenge by *Bacillus anthracis* isolates of diverse geographical origin. Vaccine **19:**3241–3247.
23. **Firoved, A. M., G. F. Miller, M. Moayeri, R. Kakkar, Y. Shen, J. F. Wiggins, E. M. McNally, W. J. Tang, and S. H. Leppla.** 2005. *Bacillus anthracis* edema toxin causes extensive tissue lesions and rapid lethality in mice. Am. J. Pathol. **167:**1309–1320.
24. **Flannigan, K. A., S. H. Hennigan, H. H. Vogelbacker, J. S. Gots, and J. M. Smith.** 1990. Purine biosynthesis in *Escherichia coli* K12: structure and DNA sequence studies of the *purHD* locus. Mol. Microbiol. **4:**381–392.
25. **Friedlander, A. M.** 2000. Anthrax: clinical features, pathogenesis, and potential biological warfare threat. Curr. Clin. Top. Infect. Dis. **20:**335–349.
26. **Grenha, R., V. M. Levdikov, M. J. Fogg, E. V. Blagova, J. A. Brannigan, A. J. Wilkinson, and K. S. Wilson.** 2005. Structure of purine nucleoside phosphorylase (DeoD) from *Bacillus anthracis*. Acta Crystallogr. Sect. F Struct. Biol. Cryst. Commun. **61:**459–462.
27. **Grinberg, L. M., F. A. Abramova, O. V. Yampolskaya, D. H. Walker, and J. H. Smith.** 2001. Quantitative pathology of inhalational anthrax. I. Quantitative microscopic findings. Mod. Pathol. **14:**482–495.
28. **Headrick, J. P., J. Peart, B. Hack, B. Garnham, and G. P. Matherne.** 2001. 5′-Adenosine monophosphate and adenosine metabolism, and adenosine responses in mouse, rat and guinea pig heart. Comp. Biochem. Physiol. A Mol. Integr. Physiol. **130:**615–631.
29. **Hoiseth, S. K., and B. A. Stocker.** 1981. Aromatic-dependent *Salmonella typhimurium* are non-virulent and effective as live vaccines. Nature **291:**238–239.
30. **Iványovics, G., E. Marjai, and A. Dobozy.** 1968. The growth of purine mutants of *Bacillus anthracis* in the body of the mouse. J. Gen. Microbiol. **53:**147–162.
31. **Ivins, B., P. Fellows, L. Pitt, J. Estep, J. Farchaus, A. Friedlander, and P. Gibbs.** 1995. Experimental anthrax vaccines: efficacy of adjuvants combined with protective antigen against an aerosol *Bacillus anthracis* spore challenge in guinea pigs. Vaccine **13:**1779–1784.
32. **Ivins, B. E., P. F. Fellows, and G. O. Nelson.** 1994. Efficacy of a standard human anthrax vaccine against *Bacillus anthracis* spore challenge in guinea-pigs. Vaccine **12:**872–874.
33. **Ivins, B. E., S. L. Welkos, G. B. Knudson, and S. F. Little.** 1990. Immunization against anthrax with aromatic compound-dependent (Aro^-) mutants of *Bacillus anthracis* and with recombinant strains of *Bacillus subtilis* that produce anthrax protective antigen. Infect. Immun. **58:**303–308.
34. **Jarvis, S. M., J. R. Hammond, A. R. Paterson, and A. S. Clanachan.** 1982. Species differences in nucleoside transport. A study of uridine transport and nitrobenzylthioinosine binding by mammalian erythrocytes. Biochem. J. **208:**83–88.
35. **Johansen, L. E., P. Nygaard, C. Lassen, Y. Agerso, and H. H. Saxild.** 2003. Definition of a second *Bacillus subtilis pur* regulon comprising the *pur* and *xpt-pbuX* operons plus *pbuG*, *nupG* (*yxjA*), and *pbuE* (*ydhL*). J. Bacteriol. **185:**5200–5209.
36. **Kappock, T. J., S. E. Ealick, and J. Stubbe.** 2000. Modular evolution of the purine biosynthetic pathway. Curr. Opin. Chem. Biol. **4:**567–572.
37. **Kim, Y. R., S. E. Lee, C. M. Kim, S. Y. Kim, E. K. Shin, D. H. Shin, S. S. Chung, H. E. Choy, A. Progulske-Fox, J. D. Hillman, M. Handfield, and J. H. Rhee.** 2003. Characterization and pathogenic significance of *Vibrio vulnificus* antigens preferentially expressed in septicemic patients. Infect. Immun. **71:**5461–5471.
38. **Klarsfeld, A. D., P. L. Goossens, and P. Cossart.** 1994. Five *Listeria monocytogenes* genes preferentially expressed in infected mammalian cells: *plcA*, *purH*, *purD*, *pyrE* and an arginine ABC transporter gene, *arpJ*. Mol. Microbiol. **13:**585–597.
39. **Kuo, S. R., M. C. Willingham, S. H. Bour, E. A. Andreas, S. K. Park, C. Jackson, N. S. Duesbery, S. H. Leppla, W. J. Tang, and A. E. Frankel.** 2008. Anthrax toxin-induced shock in rats is associated with pulmonary edema and hemorrhage. Microb. Pathog. **44:**467–472.
40. **Little, S. F., and G. B. Knudson.** 1986. Comparative efficacy of *Bacillus anthracis* live spore vaccine and protective antigen vaccine against anthrax in the guinea pig. Infect. Immun. **52:**509–512.
41. **Lu, S., C. D. Smith, Z. Yang, P. S. Pruett, L. Nagy, D. McCombs, L. J. Delucas, W. J. Brouillette, and C. G. Brouillette.** 2008. Structure of nicotinic acid mononucleotide adenylyltransferase from *Bacillus anthracis*. Acta Crystallogr. Sect. F Struct. Biol. Cryst. Commun. **64:**893–898.
42. **Lyons, C. R., J. Lovchik, J. Hutt, M. F. Lipscomb, E. Wang, S. Heninger, L. Berliba, and K. Garrison.** 2004. Murine model of pulmonary anthrax: kinetics of dissemination, histopathology, and mouse strain susceptibility. Infect. Immun. **72:**4801–4809.
43. **Marquis, H., H. G. Bouwer, D. J. Hinrichs, and D. A. Portnoy.** 1993. Intracytoplasmic growth and virulence of *Listeria monocytogenes* auxotrophic mutants. Infect. Immun. **61:**3756–3760.
44. **May, M., S. Mehboob, D. C. Mulhearn, Z. Wang, H. Yu, G. R. Thatcher, B. D. Santarsiero, M. E. Johnson, and A. D. Mesecar.** 2007. Structural and functional analysis of two glutamate racemase isozymes from *Bacillus anthracis* and implications for inhibitor design. J. Mol. Biol. **371:**1219–1237.
45. **McFarland, W. C., and B. A. Stocker.** 1987. Effect of different purine auxotrophic mutations on mouse-virulence of a Vi-positive strain of *Salmonella dublin* and of two strains of *Salmonella typhimurium*. Microb. Pathog. **3:**129–141.
46. **McMurry, J., and T. P. Begley.** 2005. The organic chemistry of biological pathways. Roberts and Company Publishers, Englewood, CO.
47. **Mei, J. M., F. Nourbakhsh, C. W. Ford, and D. W. Holden.** 1997. Identification of *Staphylococcus aureus* virulence genes in a murine model of bacteraemia using signature-tagged mutagenesis. Mol. Microbiol. **26:**399–407.
48. **Meier, C., L. G. Carter, S. Sainsbury, E. J. Mancini, R. J. Owens, D. I.**

Stuart, and R. M. Esnouf. 2008. The crystal structure of UMP kinase from *Bacillus anthracis* (BA1797) reveals an allosteric nucleotide-binding site. J. Mol. Biol. **381:**1098–1105.
49. **Mendelson, I., S. Tobery, A. Scorpio, J. Bozue, A. Shafferman, and A. M. Friedlander.** 2004. The NheA component of the non-hemolytic enterotoxin of *Bacillus cereus* is produced by *Bacillus anthracis* but is not required for virulence. Microb. Pathog. **37:**149–154.
50. **Meyer, E., T. J. Kappock, C. Osuji, and J. Stubbe.** 1999. Evidence for the direct transfer of the carboxylate of N5-carboxyaminoimidazole ribonucleotide (N5-CAIR) to generate 4-carboxy-5-aminoimidazole ribonucleotide catalyzed by *Escherichia coli* PurE, an N5-CAIR mutase. Biochemistry **38:** 3012–3018.
51. **Meyer, K. F., G. Smith, L. Foster, M. Brookman, and M. Sung.** 1974. Live, attenuated *Yersinia pestis* vaccine: virulent in nonhuman primates, harmless to guinea pigs. J. Infect. Dis. **129**(Suppl.)**:**S85–S112.
52. **Mock, M., and A. Fouet.** 2001. Anthrax. Annu. Rev. Microbiol. **55:**647–671.
53. **Moir, A., and D. Smith.** 1990. The genetics of bacterial spore germination. Annu. Rev. Microbiol. **44:**531–553.
54. **Nicely, N. I., D. Parsonage, C. Paige, G. L. Newton, R. C. Fahey, R. Leonardi, S. Jackowski, T. C. Mallett, and A. Claiborne.** 2007. Structure of the type III pantothenate kinase from *Bacillus anthracis* at 2.0 Å resolution: implications for coenzyme A-dependent redox biology. Biochemistry **46:**3234–3245.
55. **Oyston, P. C., P. Russell, E. D. Williamson, and R. W. Titball.** 1996. An *aroA* mutant of *Yersinia pestis* is attenuated in guinea-pigs, but virulent in mice. Microbiology **142**(Pt. 7)**:**1847–1853.
56. **Patching, S. G., S. A. Baldwin, A. D. Baldwin, J. D. Young, M. P. Gallagher, P. J. Henderson, and R. B. Herbert.** 2005. The nucleoside transport proteins, NupC and NupG, from *Escherichia coli:* specific structural motifs necessary for the binding of ligands. Org. Biomol. Chem. **3:**462–470.
57. **Perez-Casal, J., M. G. Caparon, and J. R. Scott.** 1991. Mry, a *trans*-acting positive regulator of the M protein gene of *Streptococcus pyogenes* with similarity to the receptor proteins of two-component regulatory systems. J. Bacteriol. **173:**2617–2624.
58. **Philips, F. S., J. B. Thiersch, and A. Bendich.** 1952. Adenine intoxication in relation to in vivo formation and deposition of 2,8-dioxyadenine in renal tubules. J. Pharmacol. Exp. Ther. **104:**20–30.
59. **Polissi, A., A. Pontiggia, G. Feger, M. Altieri, H. Mottl, L. Ferrari, and D. Simon.** 1998. Large-scale identification of virulence genes from *Streptococcus pneumoniae*. Infect. Immun. **66:**5620–5629.
60. **Ristroph, J. D., and B. E. Ivins.** 1983. Elaboration of *Bacillus anthracis* antigens in a new, defined culture medium. Infect. Immun. **39:**483–486.
61. **Samant, S., H. Lee, M. Ghassemi, J. Chen, J. L. Cook, A. S. Mankin, and A. A. Neyfakh.** 2008. Nucleotide biosynthesis is critical for growth of bacteria in human blood. PLoS Pathog. **4:**e37.
62. **Schwarz, M. R., and W. O. Rieke.** 1963. The utilization in vivo of mouse nucleic acid metabolites labeled with radioactive precursor substances. Lab. Invest. **12:**92–101.
63. **Stocker, B. A., S. K. Hoiseth, and B. P. Smith.** 1983. Aromatic-dependent "*Salmonella* sp." as live vaccine in mice and calves. Dev. Biol. Stand. **53:**47–54.
64. **Twenhafel, N. A., E. Leffel, and M. L. Pitt.** 2007. Pathology of inhalational anthrax infection in the African green monkey. Vet. Pathol. **44:**716–721.
65. **Vasconcelos, D., R. Barnewall, M. Babin, R. Hunt, J. Estep, C. Nielsen, R. Carnes, and J. Carney.** 2003. Pathology of inhalation anthrax in cynomolgus monkeys (*Macaca fascicularis*). Lab. Invest. **83:**1201–1209.
66. **Welkos, S. L.** 1991. Plasmid-associated virulence factors of non-toxigenic (pX01-) *Bacillus anthracis*. Microb. Pathog. **10:**183–198.
67. **Welkos, S. L., D. Becker, A. Friedlander, and R. Trotter.** 1990. Pathogenesis and host resistance to *Bacillus anthracis*: a mouse model. Salisbury Med. Bull. **68:**49–52.
68. **Welkos, S. L., T. J. Keener, and P. H. Gibbs.** 1986. Differences in susceptibility of inbred mice to *Bacillus anthracis*. Infect. Immun. **51:**795–800.
69. **Welkos, S. L., R. W. Trotter, D. M. Becker, and G. O. Nelson.** 1989. Resistance to the Sterne strain of *B. anthracis*: phagocytic cell responses of resistant and susceptible mice. Microb. Pathog. **7:**15–35.
70. **Welkos, S. L., N. J. Vietri, and P. H. Gibbs.** 1993. Non-toxigenic derivatives of the Ames strain of *Bacillus anthracis* are fully virulent for mice: role of plasmid pX02 and chromosome in strain-dependent virulence. Microb. Pathog. **14:**381–388.
71. **Zaucha, G. M., L. M. Pitt, J. Estep, B. E. Ivins, and A. M. Friedlander.** 1998. The pathology of experimental anthrax in rabbits exposed by inhalation and subcutaneous inoculation. Arch. Pathol. Lab. Med. **122:**982–992.
72. **Zhang, Y., M. Morar, and S. E. Ealick.** 2008. Structural biology of the purine biosynthetic pathway. Cell. Mol. Life Sci. **65:**3699–3724.

Editor: S. R. Blanke